

1 **How stereochemistry influences the taste of wine:**
2 **Isolation, characterization and sensory evaluation of**
3 **lyoniresinol stereoisomers**

4
5
6
7
8 Blandine N. Cretin^{a,b}, Quentin Sallembien^{a,b}, Lauriane Sindt^{a,b}, Nicolas Daugey^c, Thierry
9 Buffeteau^c, Pierre Waffo-Teguo^d, Denis Dubourdieu^{a,b}, Axel Marchal^{a,b}

10
11
12 ^a Université de Bordeaux, ISVV, EA 4577, Unité de recherche OENOLOGIE, F-33882
13 Villenave d'Ornon, France

14 ^b INRA, ISVV, USC 1366 OENOLOGIE, 33882 Villenave d'Ornon, France

15 ^c Université de Bordeaux, UMR 5255–CNRS, Institut des Sciences Moléculaires, 351 Cours
16 de la Libération, F-33405 Talence, France

17 ^d Université de Bordeaux, ISVV, GESVAB, EA 3675, F-33882 Villenave d'Ornon, France

18
19
20
21
22 Corresponding author:

23 Axel Marchal

24 axel.marchal@u-bordeaux.fr

25 **Abstract:**

26 Wine expresses its beauty by sending a sensory message to the taster through molecules coming
27 from grapes, yeast metabolism or oak wood. Among the compounds released during barrel
28 aging, lyoniresinol has been recently reported as a relevant contributor to wine bitterness. As
29 this lignan contains three stereogenic carbons, this work aimed at investigating the influence of
30 stereochemistry on wine taste by combining analytical and sensorial techniques. First, an oak
31 wood extract was screened by Liquid Chromatography–High Resolution Mass Spectrometry to
32 target isomers separable in a symmetric environment and a diastereoisomer called *epi*-
33 lyoniresinol was isolated for the first time. Then, an original racemic resolution based on natural
34 xylose-derivatives was carried out to obtain lyoniresinol enantiomers. Chiroptical spectroscopic
35 measurements associated with theoretical calculations allowed the unambiguous determination
36 of their absolute configuration. The taste properties of all these stereoisomers revealed that only
37 one lyoniresinol enantiomer is strongly bitter whereas the other one is tasteless and the
38 diastereoisomer is slightly sweet. The presence of these three compounds was established in an
39 oaked Bordeaux wine by chiral and non-chiral chromatography, suggesting the significant
40 influence of stereochemistry on wine taste.

41

42 **Keywords:** Chiral Liquid Chromatography–High Resolution Mass Spectrometry, Vibrational
43 circular dichroism, Counter Current Chromatography, Lignan, Oak wood, Bitterness

44

45 **Highlights**

46 Targeted screening by LC–HRMS was used to search for stereoisomers of lyoniresinol.

47 *Epi*-lyoniresinol was isolated and identified for the first time in *Quercus* genus.

48 Two lyoniresinol enantiomers were separated.

49 Vibrational circular dichroism was used to determine their absolute configuration.

50 Among lyoniresinol isomers in wine, only (+)-lyoniresinol exhibits bitterness.

51 1. Introduction

52

53 Among the aesthetic pleasures in life, wine tasting plays a special role in that, unlike
54 music, poetry or paintings, wine is physically absorbed by the taster. Therefore, even though
55 cognitive processing is primordial [1], [2], the emotion caused by wine tasting is above all due
56 to direct contact between wine stimuli and the taster's sensory receptors. These stimuli are
57 volatile and non-volatile compounds that are responsible for the odors and tastes of wine,
58 respectively. The identification of such taste-active molecules has been a subject of intense
59 research for decades, demonstrating that they can be released from grapes, synthesized by
60 micro-organisms during fermentation or chemically modified during bottle storage [3]. Oak
61 wood is another source of active molecules; during barrel aging, both volatile and non-volatile
62 compounds are released from wood to wine, whose organoleptic properties are thus highly
63 modified [4]. Recently, a lignan from oak wood called lyoniresinol was shown to exhibit
64 bitterness [5]. Another study showed that lyoniresinol is present in wines aged in new oak
65 barrels at concentrations higher than its perception threshold (1.5 mg/L in white wine),
66 establishing its key contribution to the increase in bitterness observed during oak aging [6].

67 Since the presence of functional groups can modulate the sensory attributes of wine
68 molecules [7], natural derivatives of lyoniresinol have also been sought in oak wood extract.
69 Galloyl, glucosyl and xylosyl derivatives were thus discovered, some of them exhibiting
70 bitterness but with a lower intensity than lyoniresinol [6].

71 Beyond functional groups, stereochemistry also plays an important role on organoleptic
72 properties. This importance is well known for numerous volatile compounds whose absolute
73 configuration influences both the intensity and the nature of the aroma (*S*- and *R*-enantiomers
74 of limonene smell of lemon and orange, respectively [8]). Similarly, stereochemistry also
75 influences taste attributes. For the first time in 1886, Piutti isolated *d*-asparagine, the enantiomer
76 of *L*-asparagine, demonstrating that these compounds are sweet and tasteless, respectively [9].
77 After this discovery, other compounds were shown to have different taste characteristics
78 according to their stereochemistry, such as naringin diastereoisomers with their distinct
79 bitterness [10], and alapyridaine enantiomers whose dextrorotary form has a sweet taste
80 whereas the levorotary form has no taste at all [11].

81 Interestingly, lyoniresinol has three stereogenic centers, suggesting the potential
82 existence of eight stereoisomers. Among the several plant species from which lyoniresinol has
83 been isolated, it has been observed as a mixture of both *8R,8'R,7'S*- and *8S,8'S,7'R*-enantiomers

84 with variable relative abundance [12]. In *Quercus* genus oak wood, specific optical rotation
85 measurement indicated that the two enantiomers are present at similar concentrations [13].
86 Nevertheless, their individual gustatory properties have never been assessed. Furthermore,
87 some lyoniresinol diastereoisomers have been identified in various plants [14], [15], [16], [17]
88 but never in the *Quercus* genus. Nonier et al. only evoked the presence of one lyoniresinol
89 isomer in oak wood by comparing GC–MS spectra but no further investigations were carried
90 out to verify this hypothesis [18], [19].

91 Knowledge is therefore lacking about the existence of lyoniresinol isomers in oak wood
92 and their organoleptic properties. Considering the strong bitterness developed by lyoniresinol
93 in racemic mixture, the isolation, characterization and sensory study of such stereoisomers
94 might be of particular relevance.

95 For this reason, we first sought lyoniresinol diastereoisomers in oak wood extract by
96 targeted screening and Counter Current Chromatography (CCC) isolation guided by liquid
97 chromatography coupled with high resolution mass spectrometry (LC–HRMS). Then, an
98 original enantiomeric resolution was implemented by hydrolysis of natural xyloside derivatives
99 present in oak wood. Both enantiomers were isolated and their absolute configuration was
100 determined unambiguously for the first time by means of chiroptical spectroscopic
101 measurements. The gustatory properties of all the purified compounds were assessed and their
102 presence in wine aged in oak barrels was studied to investigate whether the stereochemistry of
103 lyoniresinol might influence the taste of wine and more generally the pleasure of the consumer.

104

105 **2. Materials and methods**

106

107 **2.1. Chemicals and materials**

108 Oak wood used in this study was heartwood staves of *Quercus petraea* from various
109 French forests. The staves were 2-year air-dried and then reduced to chips by the cooperage
110 industry (Seguin Moreau, Merpins, France). Two wines were used in this study: a non-oaked
111 white Bordeaux 2013 (100% Sauvignon blanc, 13% vol. alc.) for sensory tests and a red
112 Margaux 2012 (90% Cabernet Sauvignon and 10% Merlot, 13.5% vol. alc.) aged in new French
113 oak barrels for 15 months for chemical analysis.

114 All solvents were HPLC grade (VWR International, Pessac, France) except acetonitrile
115 used for HRMS analysis (Optima® LCMS grade, Fisher Scientific, Fair Lawn, USA) and
116 deionized water (MilliQ, Millipore, Bedford, USA). Lyoniresinol, lyoniside ((+)-lyoniresinol

117 9'-O- β -xylopyranoside) and nudiposide ((-)-lyoniresinol 9'-O- β -xylopyranoside) were isolated
118 as described previously by Marchal et al., 2014 [6].

119

120 **2.2. Preparation of pre-purified oak wood extract**

121 Oak wood extract was obtained from a hydro-alcoholic solution (50:50; EtOH/H₂O) of
122 wood chips (250 g/L) for two weeks at room temperature. After a 0.45 μ m filtration, the hydro-
123 alcoholic solution was concentrated in vacuo to remove ethanol. The aqueous solution was
124 extracted three times with 200 mL of ethyl acetate (EtOAc). The combined organic layers were
125 evaporated to dryness, suspended in water and freeze-dried to obtain a brownish free-flowing
126 powder of EtOAc prepurified extract (1.9 g).

127

128 **2.3. LC–HRMS analysis**

129 The LC–HRMS apparatus consisted of an HTC PAL autosampler (CTC Analytics AG,
130 Zwingen, Switzerland), an Accela U-HPLC system with quaternary pumps and an Exactive
131 Orbitrap mass spectrometer equipped with a heated electrospray ionization HESI I probe (both
132 from Thermo Fisher Scientific, Les Ulis, France). Liquid chromatography separation was
133 carried out on a C18 column (Hypersil Gold 2.1 mm \times 100 mm, 1.9 μ m particle size, Thermo
134 Fisher Scientific) with water (Eluent A) and acetonitrile (Eluent B) as mobile phases. The flow
135 rate was set at 600 μ L/min and the injection volume was 5 μ L. Eluent B varied as follows: 0
136 min, 14%; 0.5 min, 14%; 1.5 min, 19%; 2 min, 19%; 4.5 min, 38%; 4.6 min, 98%; 6.9 min,
137 98%; 7 min, 14%; 8.6 min, 14%. Chiral chromatography analysis were performed on a
138 Chiralpak® IB-3 column (2.1 mm \times 150 mm, 3 μ m particle size) with a flow rate set at 300
139 μ L/min and an isocratic elution mode (water/acetonitrile; 80:20; v/v).

140 Mass acquisitions were performed in negative Fourier transform mass spectrometry
141 (FTMS) ionization mode. The chromatographic conditions as well as the ionization and
142 spectrometric parameters are described in Supplementary Data.

143

144 **2.4. Centrifugal partition chromatography fractionation**

145 The detailed description of the Centrifugal partition chromatography (CPC) apparatus,
146 its preparation and the procedure implemented for choosing the system are presented in
147 Supplementary Data. The quaternary system (*n*-heptane/ethyl acetate/acetonitrile/water
148 1:4:1.29:4 v/v) was used to fractionate the EtOAc prepurified extract in a 100 mL rotor. For
149 each injection, the extract (0.95 g) was dissolved in 10 mL of a mixture consisting of upper and
150 lower phases (4 mL and 6 mL, respectively) of the system, 0.45 μ m filtered and injected. The

151 experiment was performed in ascending mode at 2500 rpm with a 10 mL/min flow rate for 45
152 min. The Spot prep fraction collector was set at 1 tube/min. Every five CPC tubes, an aliquot
153 (10 μ L) was taken, evaporated, dissolved in 1 mL of water/methanol 95:5 and analyzed by LC–
154 HRMS to constitute a fraction enriched in compound **2**. To obtain such a fraction, CPC tubes
155 were pooled, evaporated in vacuo, suspended in water and freeze-dried.

156

157 **2.5. Preparative High Performance Liquid Chromatography purification**

158 The details of the apparatus and procedures used for High Performance Liquid
159 Chromatography (HPLC) purification are presented in Supplementary Data. For each injection,
160 aliquots (25–40 mg) of samples to be purified were introduced manually into the system.
161 Chromatographic peaks were collected manually just downstream the UV detector. Samples
162 obtained after successive injections were pooled, evaporated in vacuo to remove acetonitrile
163 and freeze-dried twice.

164

165 **2.6. Racemic resolution of lyoniresinol enantiomers**

166 Lyoniside (57.4 mg) and nudiposide (58.6 mg) were separately solubilized in a 4 mol
167 L⁻¹ TFA solution and placed under reflux at 80 °C. Experiments were performed in parallel
168 under a nitrogen atmosphere for 14 h. After reaction, the solutions were evaporated in vacuo to
169 remove TFA traces, suspended in water and freeze-dried twice. The crude reaction mixtures
170 were purified using preparative HPLC.

171

172 **2.7. NMR experiments**

173 All 1D and 2D NMR experiments were performed on a Bruker Avance 600 NMR
174 spectrometer (¹H at 600 MHz and ¹³C at 150 MHz) equipped with a 5-mm TXI probe. All NMR
175 spectra were acquired at 300 K in methanol-*d*₄. ¹H and ¹³C chemical shifts were referenced to
176 solvent signals. Data were processed using TOPSPIN software (Bruker). Molecule assignments
177 were obtained by two-dimensional ¹H–¹H COSY, ¹H–¹H ROESY, ¹H–¹³C HSQC and ¹H–¹³C
178 HMBC experiments.

179

180 **2.8. Polarimetry**

181 A JASCO P-2000 polarimeter with a sodium emission wavelength ($\lambda = 589$ nm) was used to
182 determine the specific optical rotations of lyoniresinol stereoisomers in methanol at 293 K.

183

184 **2.9. Vibrational circular dichroism measurements**

185 Infrared (IR) and Vibrational Circular Dichroism (VCD) spectra were recorded with a
186 ThermoNicolet Nexus 670 FTIR spectrometer equipped with a VCD optical bench [20]. In this
187 optical bench, the light beam was focused by a BaF₂ lens (191 mm focal length) onto the sample,
188 passing an optical filter, a BaF₂ wire grid polarizer (Specac) and a ZnSe photoelastic modulator
189 (Hinds Instruments, Type II/ZS50). The light was focused by a ZnSe lens (38.1 mm focal
190 length) onto a 1 × 1 mm² HgCdTe (ThermoNicolet, MCTA* E6032) detector. IR and VCD
191 spectra were recorded at a resolution of 4 cm⁻¹ by co-adding 50 scans and 36000 scans (12 h
192 acquisition time), respectively. The sample was held in a fixed path length (100 μm) cell with
193 BaF₂ windows. IR and VCD spectra of lyoniresinol enantiomers **1a** and **1b** were measured in
194 DMSO-*d*₆ at a concentration of 50 mM. In all experiments, the photoelastic modulator was
195 adjusted for a maximum efficiency at 1400 cm⁻¹. Calculations were done with the standard
196 ThermoNicolet software, using Happ and Genzel apodization, de-Haseth phase correction, and
197 a zero-filling factor of one. Calibration spectra were recorded using a birefringent plate (CdSe)
198 and a second BaF₂ wire grid polarizer, according to a published procedure [21].

199

200 **2.10. Density functional theory calculations**

201 The calculation of the IR and VCD spectra began with a thorough analysis of the
202 conformational freedom of the lyoniresinol molecule. This involved exploring the entire
203 conformational energy surface of the (8*R*,8'*R*,7'*S*)-enantiomer (**1a**) and carrying out semi-
204 empirical RM1 [22] calculations with the simulated annealing technique [23], as both
205 implemented in the Ampac package [24], of the relative energies of conformers found in the
206 various local minima of this surface. Energy minima were sought in two stages: (i) a non-local
207 search focused on the main dihedral angles and (ii) a local energy relaxation of the whole
208 degrees of freedom for each of the minima collected at stage (i). Seventy-two conformers within
209 roughly 3 kcal/mol of the lowest energy conformer were kept for further density functional
210 theory (DFT) calculations.

211 The geometry optimizations, vibrational frequencies, absorption and VCD intensities
212 were calculated with the Gaussian 09 program [25] on the DELL cluster of the MCIA
213 computing center at the University of Bordeaux. Calculations of the optimized geometry of 72
214 conformers of (8*R*,8'*R*,7'*S*)-lyoniresinol were performed at the density functional theory level
215 using the B3PW91 functional and the 6-311G** basis set. Vibrational frequencies, IR and VCD
216 intensities were calculated at the same level of theory using the magnetic field perturbation
217 method with gauge-invariant atomic orbitals [26]. The spectra were calculated for the isolated
218 molecule in vacuo. For comparison with the experiment, the calculated frequencies were scaled

219 by 0.968 and the calculated intensities were converted to Lorentzian bands with a half-width of
220 7 cm^{-1} . The experimental IR spectra of the (+)- and (-)-lyoniresinol as well as the predicted IR
221 spectrum of (8*R*, 8'*R*, 7'*S*)-lyoniresinol are reported in Supplementary Data (Fig. S7).

222 All spectroscopic data concerning **1a**, **1b** and **2** are available in Supplementary material.

223

224 **2.11. Sensory analysis of purified compounds**

225 Tasting sessions took place in a specific room air-conditioned at 20 °C and equipped
226 with individual booths and normalized glasses. Compounds were tasted in a hydro-alcoholic
227 solution composed of pure and demineralized water (eau de source de Montagne, Laqueuille,
228 France) and distilled ethanol, as well as in a white non-oaked wine. Compounds were dissolved
229 at 2 mg L^{-1} in a 12% vol. alc. hydro-alcoholic solution. Samples were tasted by five wine-
230 tasting experts. They were asked to describe the gustatory perception of each compound using
231 wine tasting vocabulary and to evaluate the bitterness intensity on a scale from 0 (not detectable)
232 to 5 (strongly detectable).

233

234 **3. Results and discussion**

235

236 **3.1. Evidence and purification of one lyoniresinol isomer**

237 Owing to differences in their physico-chemical properties, structural isomers and
238 diastereoisomers can be separated in a non-chiral environment. Consequently, ultra high-
239 performance liquid chromatography (U-HPLC) equipped with a classical C18 column was
240 coupled with Fourier Transform mass spectrometry (FTMS) to search for such isomers of
241 lyoniresinol by targeting the m/z 419.1712 corresponding to its deprotonated ion $\text{C}_{22}\text{H}_{27}\text{O}_8^-$.
242 This MS technique is very efficient for screening unknown compounds in complex matrixes.
243 Indeed, its high sensitivity together with the specificity afforded by accurate mass measurement
244 allowed its implementation in full scan mode, whereas the use of triple-quadrupole
245 spectrometers in multiple reaction monitoring (MRM) mode requires preliminary optimization
246 of transitions with pure compounds.

247 As shown in Fig. 1, the analysis of a hydro-ethanolic oak wood extract showed two
248 peaks at retention times of 2.69 and 2.85 min in the extracted ion chromatogram (XIC) recorded
249 in a 5 ppm window around m/z 419.1712. The gradient was optimized for a distinct separation
250 of the two signals. The analysis of the same sample boosted with a stock solution of pure
251 lyoniresinol resulted in an increase in the intensity of the dominant peak at the retention time

252 of 2.69 min, establishing that this first peak was lyoniresinol (compound **1**). The existence of a
253 second peak at a retention time of 2.85 min highlighted the existence of an isomer of
254 lyoniresinol in the oak wood extract (compound **2**). Such an isomer has never been reported in
255 oak wood. To purify this new isomer, an LC–HRMS-guided procedure was developed.

256 After AcOEt extraction to eliminate the most polar compounds and in particular
257 glycosylated lignans, the prepurified AcOEt extract was further fractionated by centrifugal
258 partition chromatography (CPC). An appropriate solvent system was chosen to maximize the
259 differences between the calculated partition coefficients *K_d*. The system *n*-heptane/ethyl
260 acetate/acetonitrile/water 1:4:1.29:4 v/v gave the best results with *K_d* of 1.7 and 1.1 for
261 compounds **1** and **2**, respectively. Nevertheless, considering these values, the two compounds
262 are not likely to be completely separated, but a fraction enriched in the targeted compound
263 might be obtained. CPC fractionation using the 100 mL rotor allows the injection of up to 1 g
264 of AcOEt prepurified extract with a minimum consumption of solvent for 45 min. Two
265 successive injections were performed to process the whole extract. After LC–HRMS analyses,
266 CPC tubes were pooled and freeze-dried to make one enriched fraction of lyoniresinol isomer.
267 This fraction was then submitted to preparative HPLC with an optimized gradient for compound
268 separation. The purity of the isolated lyoniresinol isomer was found to be higher than 95% by
269 LC–HRMS analysis.

270

271 **3.2. Structural and sensory analysis of lyoniresinol diastereoisomer**

272 To elucidate the chemical structure of this lyoniresinol isomer, 1D and 2D NMR
273 experiments were performed (Supplementary Data, Figs. S1 to S3). ¹H and ¹³C NMR signals
274 were assigned as presented in Supplementary Data (Table S1) and were compared to those
275 reported in the literature for *epi*-lyoniresinol [17]. In particular, the relative configuration of the
276 stereogenic carbons (C-8, C-7', and C-8') was established by ROESY. The ROEs correlation
277 between H-2'(H-6')/H-8 and H-7'/H-8' indicated that H-7' and H-8' are *cis*-orientated (cofacial).
278 Moreover, the absence of a cross peak between H-8/H-8' suggested that these protons were
279 *trans*-orientated (Supplementary Data, Fig. S3). Thus, these results established that the purified
280 molecule is a diastereoisomer of lyoniresinol (compound **2**) whose relative configuration was
281 concluded to differ from lyoniresinol by the epimerization on C-7' position, as shown in Fig. 2.
282 This diastereoisomer has already been identified in the bark of *Aegle marmelos* by Ohashi et al.
283 [17], but we report here for the first time its identification in *Quercus* genus.

284 The specific optical rotation of *epi*-lyoniresinol **2** was measured to be –39 and its
285 analysis by LC–HRMS using a chiral column revealed the presence of two chromatographic

286 peaks (Supplementary Data, Figure S4). Based on these observations and on literature data
287 showing a specific optical rotation of -140.8 for $(-)$ -*epi*-lyoniresinol [17], *epi*-lyoniresinol **2**
288 appeared to be present in oak wood as a mixture of both its enantiomeric forms but with an
289 excess of the levorotatory form.

290 Unlike lyoniresinol [27], the presence of *epi*-lyoniresinol in wine has not been described
291 until now. Fig. S5 in Supplementary Data presents extracted ion chromatograms (XIC) obtained
292 in an oaked red wine for an m/z ratio specific to lyoniresinol and *epi*-lyoniresinol. Two signals
293 were detected at 2.64 and 2.80 min. These retention times were similar (0.05 min lower) to
294 those measured for oak wood extract in a 5 ppm window, demonstrating the presence of both
295 compounds **1** and **2** in oaked red wine. Consequently, this study is the first to identify **epi**-
296 lyoniresinol in wine.

297 Owing to the sensory properties of lyoniresinol **1** with a perception threshold of
298 bitterness evaluated at 1.5 mg/L by Marchal et al. 2014 [6], we decided to analyze the taste
299 perception of *epi*-lyoniresinol. Therefore, *epi*-lyoniresinol **2** was tasted at 2 mg/L in a 12% vol.
300 alc. hydro-alcoholic as well as in a non-oaked white wine. Experts described its taste as not
301 bitter and barely slightly sweet in comparison to the control medium solution.

302 Considering these results and the lower amount of *epi*-lyoniresinol compared to
303 lyoniresinol both in oak wood and oaked wine, *epi*-lyoniresinol appeared unlikely to influence
304 the taste of wine. Consequently, no further investigations were conducted on this compound or
305 on its enantiomeric forms.

306

307 **3.3. Enantiomeric resolution of lyoniresinol**

308 LC–HRMS analysis of an oak wood extract with a C18 column revealed the existence
309 of two diastereoisomers: lyoniresinol **1** and *epi*-lyoniresinol **2**. Nevertheless, the specific optical
310 rotation of lyoniresinol **1** was reported to be close to zero in oak wood [6] indicating a mixture
311 of two enantiomers **1a** and **1b** (Fig. 2) in the extracted compound. Thus, all sensory studies
312 concerning lyoniresinol until now have been carried out using a racemic mixture purified from
313 oak wood and the properties of each enantiomer have never been individually assessed.
314 Generally, the racemate resolution is performed using HPLC with a chiral column at a
315 preparative scale, but such a column remains very costly. Another approach is to derivatize the
316 enantiomers previously with the same chiral moiety in order to obtain diastereoisomers, which
317 can be separated by non-chiral chromatography. After separation, each diastereoisomer can be
318 hydrolyzed to obtain the targeted enantiomers.

319 In this study, we decided to resolve the lyoniresinol racemic mixture by separation and
320 hydrolysis of natural derivatized diastereoisomers. Indeed, previous studies have established
321 the presence in oak wood of lyoniside **3** and nudiposide **4**, two native xylopyranoside-
322 derivatives of (+)- and (-)-lyoniresinol, respectively [28], [29]. For this purpose, lyoniside **3**
323 and nudiposide **4** purified as previously described [6] were heated in acidic conditions under
324 inert atmosphere to hydrolyze the acetal formed between the xylose aldehyde and the primary
325 alcohol (C9') of lyoniresinol, as shown in Fig. 3. TFA was used to acidify the solution since it
326 could be easily removed *in vacuo* from the crude reaction mixture.

327 The hydrolysis was monitored by LC–HRMS in order to ensure a complete reaction
328 with a total disappearance of lyoniside **3** and nudiposide **4** through xylopyranoside cleavage
329 from the genin, leading to lyoniresinol enantiomers **1a** and **1b** and xylopyranoside by-products
330 (Supplementary Data, Fig. S6).

331 Preparative HPLC was performed on each crude reaction mixture to purify **1a** and **1b**
332 by removing all by-products. The percentage yield of the purification of (+)- and (-)-
333 lyoniresinol enantiomers was 44.6% and 43.5%, respectively. Each purified enantiomer was
334 analyzed by chiral liquid chromatography using an analytical chiral column. As shown in Fig.
335 4, (±)-lyoniresinol **1** injection revealed two peaks at 5.88 min and 7.16 min, while the purified
336 (+)- and (-)-lyoniresinol enantiomers each presented only one peak at 5.92 min and 7.17 min,
337 respectively, confirming the efficiency of the racemic resolution.

338

339 **3.4. Unambiguous determination of the absolute configurations of lyoniresinol** 340 **enantiomers**

341 1D and 2D NMR experiments were performed on each enantiomer to confirm their
342 relative configuration. ¹H NMR spectra of (+)- and (-)-lyoniresinol enantiomers superimposed
343 on that of (±)-lyoniresinol **1** (Supplementary Data, Fig. S1) and the NMR data (Supplementary
344 Data, Table S1) were identical to those reported in the literature for lyoniresinol [28], [30], [31],
345 [32]. The relative configuration of **1** was established on the basis of ROEs correlations between
346 protons H-2'(H-6')/H-8' and H-7'/H-8, suggesting that H-7' and H-8' are *trans*-orientated and
347 that H-7' and H-8 are cofacial (Supplementary Data, Fig. S2).

348 Specific optical rotation of each enantiomer was measured to be +43 and -45. These
349 values are similar with opposite signs, confirming their enantiomeric relationship. Since the
350 two enantiomers of lyoniresinol had been successfully isolated, we decided to determine their
351 absolute configurations.

352 The absolute configuration of (+)-lyoniresinol has been previously proposed to be
353 (8*R*,8'*R*,7'*S*)-(+)-lyoniresinol by degradation reactions and comparison with known compounds
354 [30], [33]. Nevertheless, the absolute configuration of lyoniresinol has never been confirmed
355 by chiroptical spectroscopic experiments (electronic or vibrational circular dichroism)
356 associated with theoretical calculations. In this study, we used vibrational circular dichroism
357 (VCD) which is a well-established method for determining the absolute configuration and
358 conformation of chiral molecules in solution [34]. The method entails comparison of measured
359 VCD spectra with the spectrum calculated at the density functional theory (DFT) level for a
360 specified absolute configuration [35]. Because enantiomers have a VCD band of opposite sign
361 for each vibrational mode, the VCD spectrum provides a unique rich signature of the absolute
362 configuration.

363 The VCD spectra of the two enantiomers of lyoniresinol were recorded in DMSO-*d*₆ at
364 a concentration of 50 mM and are reported in Fig. 5. The two spectra are opposite with respect
365 to the baseline, confirming that the two molecules are enantiomers. Theoretical calculation of
366 the (8*R*,8'*R*,7'*S*)-lyoniresinol (compound **1a** in Fig. 2) was performed to determine the absolute
367 configuration of (+)- and (-)-lyoniresinol. The conformational analysis of **1a** was carried out
368 initially by using semi-empirical RM1 calculations with the simulated annealing technique.
369 Seventy-two conformers of **1a** with energies within 3 kcal/mol of the lowest energy conformer
370 were kept. Subsequently, the 72 RM1 conformations of **1a** were optimized by using DFT at the
371 B3PW91/6-311G** level. Harmonic vibrational frequencies were calculated at the same level
372 to confirm that all structures were stable conformations and to enable free energies to be
373 calculated. The VCD spectrum predicted on the basis of the relative populations of (8*R*,8'*R*,7'*S*)-
374 lyoniresinol was compared to the experimental VCD spectra of (+)- and (-)-lyoniresinol (Fig.
375 5). The predicted VCD spectrum of (8*R*,8'*R*,7'*S*)-lyoniresinol isomer reproduced fairly well the
376 intensity and the sign of most bands observed in the experimental spectrum of (+)-lyoniresinol,
377 confirming the (8*R*,8'*R*,7'*S*)-(+)-lyoniresinol absolute configuration proposed by Kato [30],
378 [33].

379

380 **3.5. Gustatory properties of enantiomers and impact on wine taste**

381 To measure the gustatory impact of each lyoniresinol enantiomer on the bitter perception
382 of their racemic mixture **1**, enantiomers **1a** and **1b** were tasted at 2 mg/L in a 12% vol. alc.
383 hydro-alcoholic solution and compared to the control medium solution. The same
384 concentrations were tasted in a non-oaked white wine. Experts described for the first time that
385 lyoniresinol **1a** exhibited a strong bitterness equivalent to the bitterness of (±)-lyoniresinol **1** at

386 4 mg/L, while lyoniresinol **1b** exhibited no taste. Thus, the bitterness of (\pm)-lyoniresinol **1**
387 comes from that of (+)-lyoniresinol **1a** while (-)-lyoniresinol **1b** is not involved. Finally, an
388 oaked Margaux wine was analyzed by LC–HRMS equipped with a chiral column to search for
389 the presence of lyoniresinol enantiomers. The XIC for an m/z ratio specific to lyoniresinol
390 showed two peaks at 5.94 and 7.15 min corresponding to lyoniresinol enantiomers **1a** and **1b**,
391 respectively (Fig. 6). Analysis of spiked samples confirmed that both (+)-lyoniresinol **1a** and
392 (-)-lyoniresinol **1b** were present in this red oaked wine with a relative abundance similar to that
393 observed in oak wood. In view of these results and the gustatory properties of both enantiomers,
394 it appears that only (+)-lyoniresinol **1a** is likely to influence the taste of wine by increasing its
395 bitterness.

396

397 **4. Conclusion**

398

399 This study focused on the use of analytical techniques to highlight the relationship
400 between stereochemistry and the organoleptic properties of lyoniresinol. A diastereoisomer,
401 *epi*-lyoniresinol, was identified for the first time in *Quercus* genus using a CCC isolation
402 procedure guided by LC–HRMS. Moreover, two enantiomers of lyoniresinol were separated by
403 a racemic resolution from natural derivatives. This original approach appears promising for
404 natural products since it is cheaper than chiral separation and more compatible with trends in
405 green chemistry than enantiospecific synthesis. This racemic resolution allowed for the first
406 time the unambiguous determination of the absolute configuration of the two enantiomers by
407 means of VCD measurements associated with DFT calculations. The presence of all these
408 lyoniresinol stereoisomers was established in oaked wine by LC–HRMS analysis. Finally,
409 sensory analyses were carried out to determine their gustatory properties. Whereas (+)-
410 lyoniresinol exhibited strong bitterness, its enantiomer was tasteless and *epi*-lyoniresinol was
411 slightly sweet. These results demonstrate that stereochemistry strongly influences the taste of
412 wine compounds and subsequently the perception of consumers.

413

414 **Acknowledgments**

415 NMR experiments were performed at the Plateforme Métabolome-Fluxome, Centre de
416 Génomique Fonctionnelle de Bordeaux, Bordeaux, France. Blandine Cretin's grant is supported
417 by Fondation Jean Poupelain. The authors would like to acknowledge the Conseil
418 Interprofessionnel des Vins de Bordeaux, France AgriMer, Seguin-Moreau cooperage and

419 Rémy-Martin for funding this project. They thank Anastasia Bouzdine for her technical
420 assistance and Ray Cooke for proofreading the manuscript.

421 **References**

- 422 [1] F. Brochet, D. Dubourdieu, Wine descriptive language supports cognitive specificity of
423 chemical senses, *Brain Lang.* 77 (2001) 187-196.
- 424 [2] L. Pazart, A. Comte, E. Magnin, J.-L. Millot, T. Moulin, An fMRI study on the influence of
425 sommeliers' expertise on the integration of flavor, *Front. Behav. Neurosci.* 8 (2014) 358.
- 426 [3] P. Ribereau-Gayon, Y. Glories, A. Maujean, d. Dubourdieu, *Handbook of Enology, the*
427 *Chemistry of Wine Stabilization and Treatments*, second ed., Wiley, Chichester, England, 2006.
- 428 [4] T. Garde-Cerdan, C. Ancín-Azpilicueta, Review of quality factors on wine ageing in oak
429 barrels, *Trends Food Sci. Technol.* 17 (2006) 438-447.
- 430 [5] A. Marchal, P. Waffo-Teguo, E. Genin, J.M. Merillon, D. Dubourdieu, Identification of new
431 natural sweet compounds in wine using centrifugal partition chromatography-gustatometry and
432 Fourier transform mass spectrometry, *Anal. Chem.* 83 (2011) 9629-9637.
- 433 [6] A. Marchal, B.N. Cretin, L. Sindt, P. Waffo-Teguo, D. Dubourdieu, Contribution of oak
434 lignans to wine taste: chemical identification, sensory characterization and quantification,
435 *Tetrahedron* 71 (2015) 3148-3156.
- 436 [7] A. Marchal, E. Genin, P. Waffo-Teguo, A. Bibes, G. Da Costa, J.-M. Merillon, D.
437 Dubourdieu, Development of an analytical methodology using Fourier transform mass
438 spectrometry to discover new structural analogs of wine natural sweeteners, *Anal. Chim. Acta*
439 853 (2015) 425-434.
- 440 [8] T. Clarin, S. Sandhu, R. Apfelbach, Odor detection and odor discrimination in subadult and
441 adult rats for two enantiomeric odorants supported by c-fos data, *Behav. Brain Res.* 206 (2010)
442 229-235.
- 443 [9] A. Piutti, Una nuova specie di asparagine, L'Orosi, G. *Chim. Farm. Sci. Affini* (1886) 198-
444 202.
- 445 [10] W. Gaffield, R.E. Lundin, B. Gentili, R.M. Horowitz, C-2 stereochemistry of naringin and
446 its relation to taste and biosynthesis in maturing grapefruit, *Bioorg. Chem.* 4 (1975) 259-269.
- 447 [11] H. Ottinger, T. Soldo, T. Hofmann, Discovery and structure determination of a novel
448 maillard-derived sweetness enhancer by application of the comparative taste dilution analysis
449 (cTDA), *J. Agric. Food Chem.* 51 (2003) 1035-1041.
- 450 [12] M.D.A. Rahman, T. Katayama, T. Suzuki, T. Nakagawa, Stereochemistry and biosynthesis
451 of (p)-lyoniresinol, a syringyl tetrahydronaphthalene lignan in *Lyonia ovalifolia* var. *elliptica* I:
452 isolation and stereochemistry of syringyl lignans and predicted precursors to (p)-lyoniresinol
453 from wood, *J. Wood Sci.* 53 (2007) 161-167.

- 454 [13] K. Nabeta, J. Yonekubo, M. Miyake, Phenolic compounds from the heartwood of
455 European oak (*Quercus robur* L.) and brandy, J. Jpn. Wood Res. Soc. 33 (1987) 408-415.
- 456 [14] S.K. Sadhu, P. Phattanawasin, M.S.K. Choudhuri, T. Ohtsuki, M. Ishibashi, A new lignan
457 from *Aphanamixis polystachya*, J. Nat. Med. 60 (2006) 258-260.
- 458 [15] J. Zhu, J. Ren, J. Qin, X. Cheng, Q. Zeng, F. Zhang, S. Yan, H. Jin, W. Zhang,
459 Phenylpropanoids and lignanoids from *Euonymus acanthocarpus*, Arch. Pharmacol Res. 35
460 (2012) 1739-1747.
- 461 [16] E.J. Jeong, J.H. Cho, S.H. Sung, S.Y. Kim, Y.C. Kim, Inhibition of nitric oxide production
462 in lipopolysaccharide-stimulated RAW264.7 macrophage cells by lignans isolated from
463 *Euonymus alatus* leaves and twigs, Bioorg. Med. Chem. Lett. 21 (2011) 2283-2286.
- 464 [17] K. Ohashi, H. Watanabe, Y. Okumura, T. Uji, I. Kitagawa, Indonesian Medicinal Plants.
465 XII. Four Isomeric Lignan-Glucosides from the Bark of *Aegle marmelos* (Rutaceae), Chem.
466 Pharm. Bull. 42 (1994) 1924-1926.
- 467 [18] M.-F. Nonier, N. Vivas, N. Vivas de Gaulejac, E. Fouquet, Origin of brown discoloration
468 in the staves of oak used in cooperage e Characterization of two new lignans in oak wood
469 barrels, C. R. Chim. 12 (2009) 291-296.
- 470 [19] N. Vivas, Recherches sur la qualité du chêne français de tonnellerie (*Q. petraea* Liebl., *Q.*
471 *robur* L.) et sur les mécanismes d'oxydoréduction des vins rouges au cours de leur élevage en
472 barriques Sciences biologiques et médicales, in: Œnologie ampélogie, Université de
473 Bordeaux 2, 1997.
- 474 [20] T. Buffeteau, F. Lagugne-Labarthet, C. Sourisseau, Vibrational circular dichroism in
475 general anisotropic thin solid films: measurement and theoretical approach, Appl. Spectrosc.
476 59 (2005) 732-745.
- 477 [21] L.A. Nafie, D.W. Vidrine, in: J.R. Ferraro, L.J. Basile (Eds.), Fourier Transform Infrared
478 Spectroscopy, Academic Press, New York, 1982.
- 479 [22] G.B. Rocha, R.O. Freire, A.M. Simas, J.J.P. Stewart, RM1: a reparameterization of AM1
480 for H, C, N, O, P, S, F, Cl, Br, and I, J. Comput. Chem. 27 (2006) 1101-1111.
- 481 [23] F. Bockisch, D. Liotard, J.C. Rayez, B. Duguay, Simulated annealing to locate various
482 stationary points in semiempirical methods, Int. J. Quantum Chem. 44 (1992) 619-642.
- 483 [24] Semichem, AMPAC-8. KS, Semichem, 2004.
- 484 [25] M.J. Frisch, G.W. Trucks, H.B. Schlegel, G.E. Scuseria, M.A. Robb,
485 J.R. Cheeseman, G. Scalmani, V. Barone, B. Mennucci, G.A. Petersson,
486 H. Nakatsuji, M. Caricato, X. Li, H.P. Hratchian, A.F. Izmaylov, J. Bloino,
487 G. Zheng, J.L. Sonnenberg, M. Hada, M. Ehara, K. Toyota, R. Fukuda,

488 J. Hasegawa, M. Ishida, T. Nakajima, Y. Honda, O. Kitao, H. Nakai, T. Vreven, J. Montgomery,
489 J. A, J.E. Peralta, F. Ogliaro, M. Bearpark, J.J. Heyd, E. Brothers, K.N. Kudin, V.N. Staroverov,
490 R. Kobayashi, J. Normand, K. Raghavachari, A. Rendell, J.C. Burant, S.S. Iyengar, J. Tomasi,
491 M. Cossi, N. Rega, N.J. Millam, M. Klene, J.E. Knox, J.B. Cross, V. Bakken, C. Adamo, J.
492 Jaramillo, R. Gomperts, R.E. Stratmann, O. Yazyev, A.J. Austin, R. Cammi, C. Pomelli, J.W.
493 Ochterski, R.L. Martin, K. Morokuma, V.G. Zakrzewski, G.A. Voth, P. Salvador, J.J.
494 Dannenberg, S. Dapprich, A.D. Daniels, €O. Farkas, J.B. Foresman, J.V. Ortiz, J. Cioslowski,
495 D.J. Fox, Gaussian 09, Revision A.1, Gaussian Inc., Wallingford CT, 2009.

496 [26] J.R. Cheeseman, M.J. Frisch, F.J. Devlin, P.J. Stephens, Ab initio calculation of atomic
497 axial tensors and vibrational rotational strengths using density functional theory, Chem. Phys.
498 Lett. 252 (1996) 211-220.

499 [27] M. Moutounet, P.H. Rabier, J.L. Puech, E. Verette, J.M. Barillere, Analysis by HPLC of
500 extractable substances in oak wood. Application to a Chardonnay wine, Sci. Aliments 9 (1989)
501 35-51.

502 [28] G. Dada, A. Corbani, P. Manitto, G. Speranza, L. Lunazzi, Lignan Glycosides from the
503 heartwood of European Oak *Quercus petraea*, J. Nat. Prod. 52 (1989) 1327-1330.

504 [29] S. Inoshiri, M. Sasaki, H. Kohda, H. Otsuka, K. Yamasaki, Aromatic glycosides from
505 *Berchemia racemosa*, Phytochemistry 26 (1987) 2811-2814.

506 [30] Y. Kato, Structure of lyoniresinol (dimethoxyisolariciresinol), Chem. Pharm. Bull. 11
507 (1963) 823-827.

508 [31] X.-Y. Zhang, B.-G. Li, M. Zhou, X.-H. Yuan, G.-L. Zhang, Chemical constituents of
509 *Phacellaria compressa* Benth, J. Integr. Plant Biol. 48 (2006) 236-240.

510 [32] K. Imai, K. Yamauchi, T. Mitsunaga, Extractives of *Quercus crispula* sapwood infected
511 by the pathogenic fungus *Raffaelea quercivora* II: isolation and identification of phenolic
512 compounds from infected sapwood, J. Wood Sci. 59 (2013) 517-521.

513 [33] Y. Kato, The absolute configuration of lyoniresinol,, Chem. Pharm. Bull. 14 (1966) 1438-
514 1439.

515 [34] T.B. Freedman, X. Cao, R.K. Dukor, L.A. Nafie, Absolute configuration determination of
516 chiral molecules in the solution state using vibrational circular dichroism, Chirality 15 (2003)
517 743-758.

518 [35] P.J. Stephens, F.J. Devlin, Determination of the structure of chiral molecules using ab initio
519 vibrational circular dichroism spectroscopy, Chirality 12 (2000) 172-179.

Figures

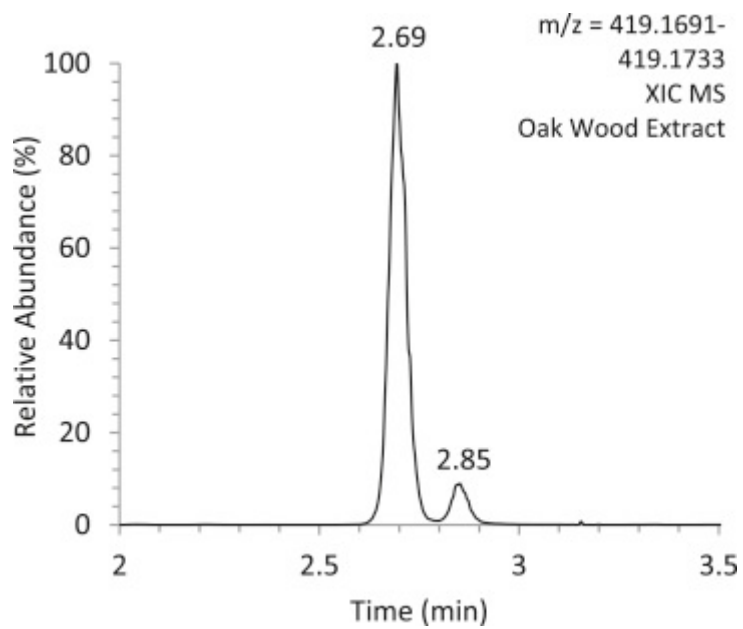


Fig. 1. Negative LC–HRMS XIC of an oak wood extract corresponding to $C_{22}H_{27}O_8^-$ ion (m/z 419.1712 with a 5 ppm accuracy).

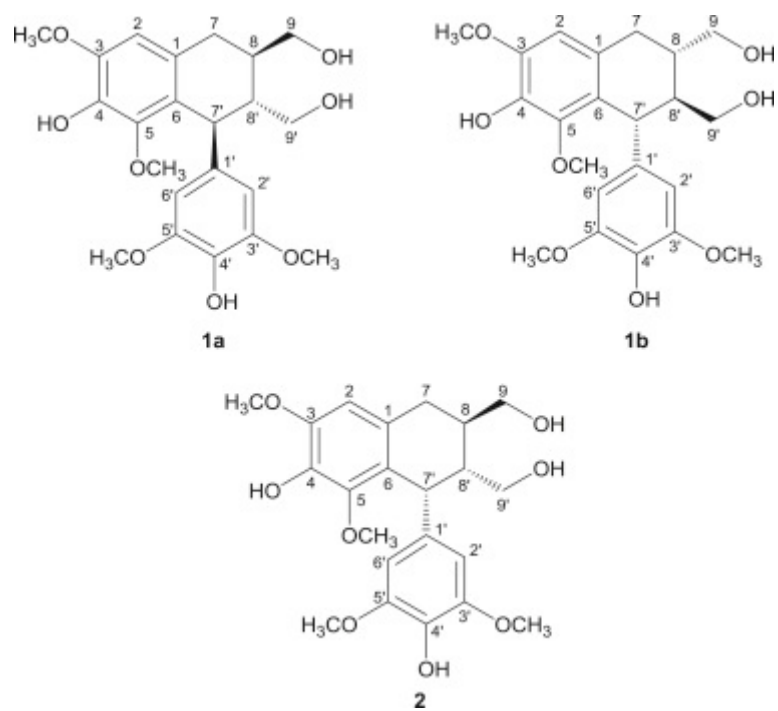


Fig. 2. Chemical structures of lyoniresinol enantiomers **1a** and **1b** (absolute configuration) and *epi*-lyoniresinol **2** (relative configuration).

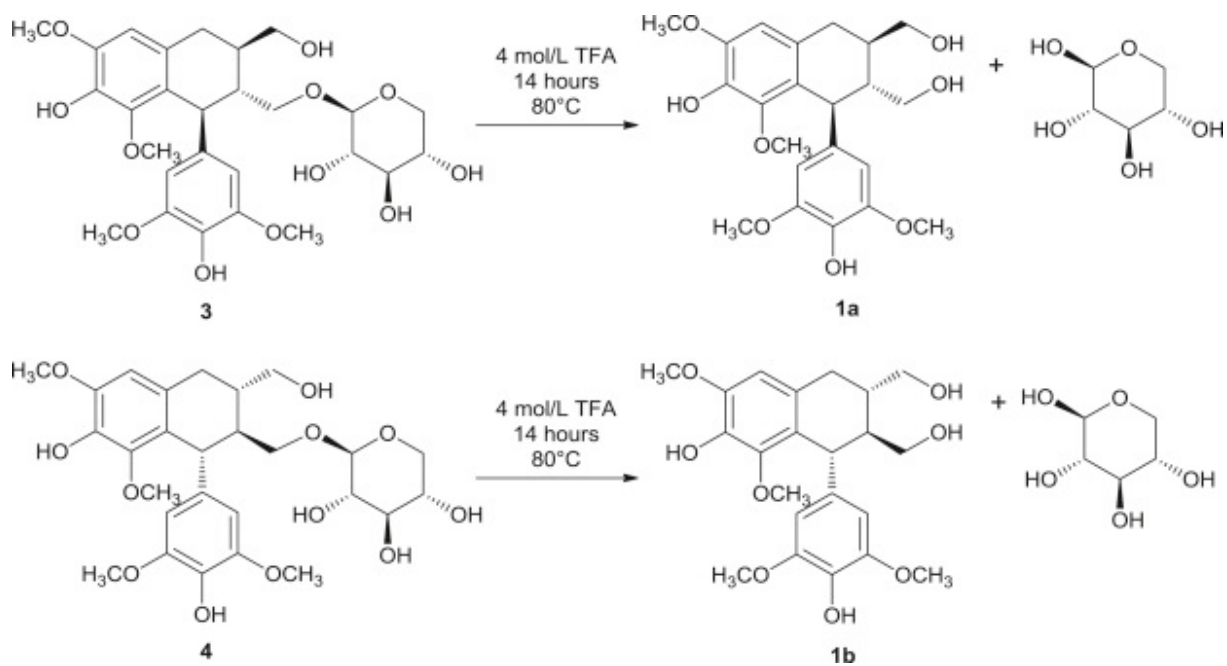


Fig. 3. Release of lyoniresinol enantiomers **1a** and **1b** by acidic hydrolysis of lyoniside **3** and nudiposide **4**, respectively.

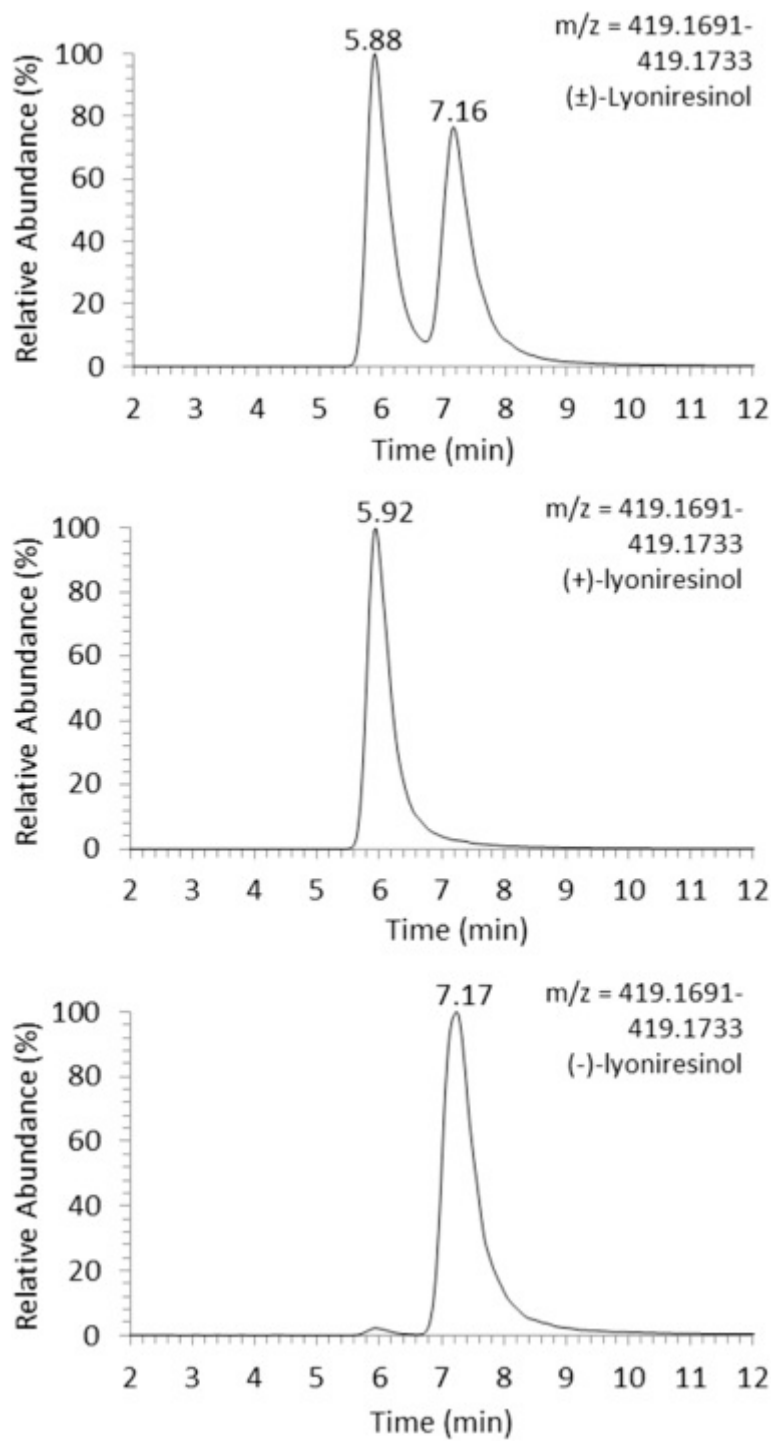


Fig. 4. LC–HRMS chromatograms of (±)-lyoniresinol, (+)-lyoniresinol and (–)-lyoniresinol (from top to bottom) on a chiral column.

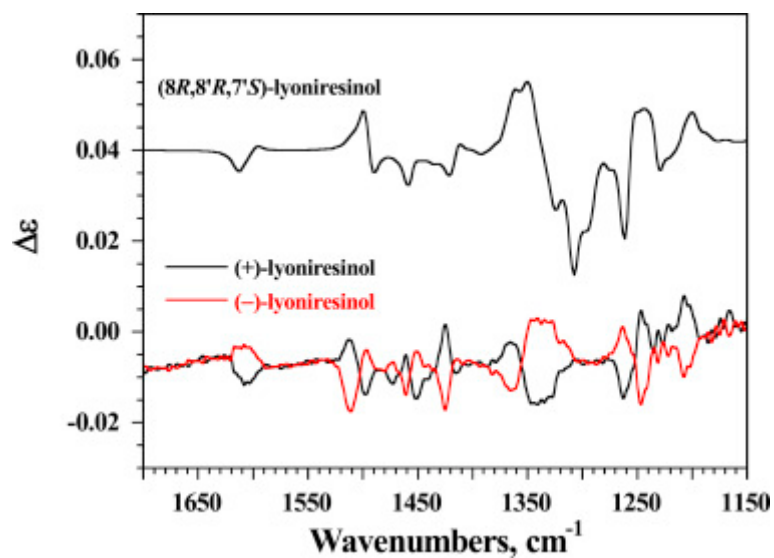


Fig. 5. Comparison of experimental VCD spectra of (+)- and (-)-lyoniresinol recorded in DMSO- d_6 solution (50 mM, 100 μm path length, bottom) with the predicted VCD spectrum of $(8R,8'R,7'S)$ -lyoniresinol isomer calculated using DFT at the B3PW91/6-311G** level (top).

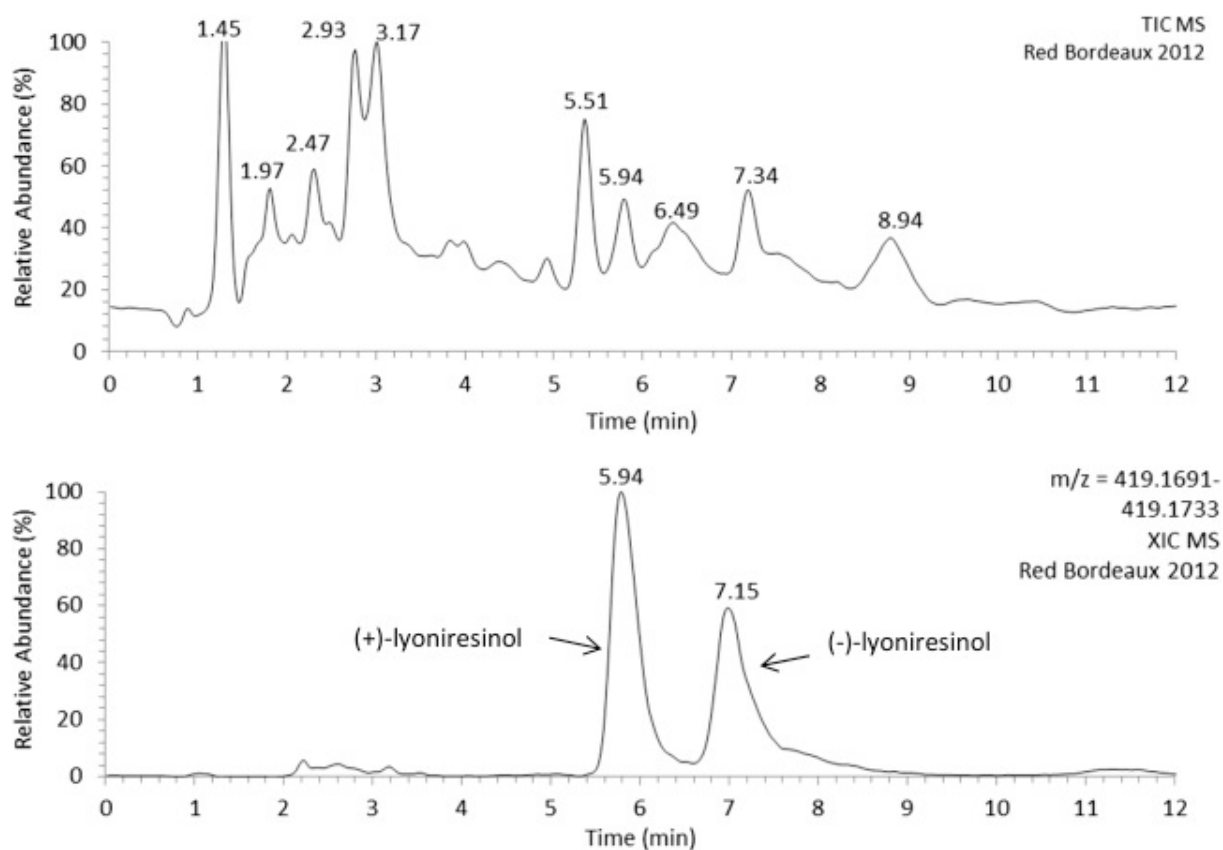


Fig. 6. Negative LC–HRMS TIC (top) and XIC corresponding to $C_{22}H_{27}O_8^-$ ion (bottom) recorded in an oaked Margaux red wine analyzed with a chiral column.